
STM Studies of Fermi-Level Pinning on the GaAs(001) Surface [and Discussion]

M. D. Pashley and G. P. Srivastava

Phil. Trans. R. Soc. Lond. A 1993 **344**, 533-543

doi: 10.1098/rsta.1993.0106

Email alerting service

Receive free email alerts when new articles cite this article - sign up in the box at the top right-hand corner of the article or click [here](#)

To subscribe to *Phil. Trans. R. Soc. Lond. A* go to:

<http://rsta.royalsocietypublishing.org/subscriptions>

STM studies of Fermi-level pinning on the GaAs(001) surface

BY M. D. PASHLEY

Philips Laboratories, North American Philips Corporation, Briarcliff Manor, New York 10510, U.S.A

This paper reviews recent scanning tunnelling microscopy (STM) studies of Fermi-level pinning on the surface of both n- and p-type GaAs(001). The samples are all grown by molecular beam epitaxy and have a $(2 \times 4)/c(2 \times 8)$ surface reconstruction. The STM has shown that on the surface of highly doped n-type GaAs(001) there is a high density of kinks in the dimer-vacancy rows of the (2×4) reconstruction. These kinks are found to be surface acceptors with approximately one electron per kink. The kinks form in exactly the required number to pin the Fermi-level of n-type GaAs(001) at an acceptor level close to mid gap, irrespective of doping level. The Fermi-level position is confirmed with tunnelling spectroscopy. No similar surface donor states are found on p-type GaAs(001). In this case Fermi-level pinning results from 'intrinsic' surface defects such as step edges. Since this intrinsic defect density is independent of doping, at high doping levels the Fermi-level on p-type GaAs(001) moves down in the band gap towards the valence band. Tunnelling spectroscopy on p-type GaAs(001) doped 10^{19} cm^{-3} with Be shows the Fermi-level to be 150 mV above the valence band maximum.

1. Introduction

Fermi-level pinning on the surface of GaAs has been studied for many years. The primary motivation is to understand the formation of the Schottky barrier when a metal is deposited onto the GaAs surface. This Schottky barrier determines the electrical contact that is made to a GaAs device structure. Since the majority of GaAs devices are grown on (001) oriented substrates, it is the GaAs(001) surface that is most important from a technology point of view. The Schottky model predicts that the height of the Schottky barrier should depend upon the work function of the metal that is deposited onto the GaAs surface. However, it is found that there is much less variation in Schottky barrier height as a function of the metal work function than the model predicts (see Rhoderick & Williams 1988). The reason for this is that states within the band gap of the GaAs surface pin the surface Fermi-level close to the middle of the band gap. The origin of these states has not been well established, and it has not been clear whether the ideal clean GaAs(001) surface has any states within the band gap.

Measurements of the surface Fermi-level and the movement of the Fermi-level as metal is deposited onto the GaAs surface are usually done using photoemission. Most of these studies start by measuring the Fermi-level position at the clean GaAs surface. The literature contains a large spread in the Fermi-level position of the clean GaAs(001) surface, ranging from close to mid gap (Spicer *et al.* 1988) up to close to the conduction band minimum for n-doped material (Viturro *et al.* 1989). It was

Phil. Trans. R. Soc. Lond. A (1993) **344**, 533–543

Printed in Great Britain

© 1993 The Royal Society

[91]

533

pointed out by Hecht (1990) that the photoemission measurement induces a surface photovoltage which tends to flatten out the bands and so make the surface Fermi-level appear artificially high in the band gap. The surface photovoltage is increased for large photon fluxes and low doping levels in the GaAs. This created uncertainty about some of the published data on the Fermi-level position on the clean GaAs(001) surface. More recent photoemission data of Mao *et al.* (1992), where the surface photovoltage did not affect the results, show the Fermi-level on the clean GaAs(001) surface to be close to the middle of the band gap.

This paper will review recent scanning tunnelling microscopy (STM) studies of Fermi-level pinning on the GaAs(001) surface (Pashley & Haberern 1991; Pashley *et al.* 1992, 1993), and bring together the results on both n- and p-type GaAs(001). It has been possible to identify the formation of a particular defect on the clean GaAs(001) surface which is responsible for pinning on the surface of n-type material. We now understand the mechanism of formation of this surface defect in some detail. Scanning tunnelling spectroscopy (STS) is able to determine the Fermi-level position and to show that the surface defects which form are charged acceptor states. Different pinning behaviour is found for n- and p-type material.

2. Structure of the GaAs(001)-(2 × 4)/c(2 × 8) surface

Before the mechanism of Fermi-level pinning can be discussed, it is necessary to consider the structure of the GaAs(001) surface. One difficulty in comparing many previous studies of pinning is that the surface structure was not always well defined. The GaAs(001) surface is highly complex with many different surface reconstructions occurring, dependent on temperature and surface stoichiometry (Drathen *et al.* 1978). In the STM studies discussed here, the GaAs were grown by molecular beam epitaxy (MBE) and had a (2 × 4)/c(2 × 8) surface reconstruction. This is the reconstruction that occurs during normal arsenic-rich growth conditions and is the best understood of all the GaAs(001) surface reconstructions.

The (2 × 4) reconstruction arises from the formation of As dimers leading to a 2 × periodicity in the $[\bar{1}10]$ direction, with the 4 × periodicity in the [110] direction arising from a regular array of As dimer-vacancies. These dimer-vacancies line up so as to produce dimer-vacancy rows extending across the surface in the $[\bar{1}10]$ direction. There are at least two forms of the (2 × 4) unit cell structure: with one dimer-vacancy and three As dimers per unit cell (Chadi 1987) and with two dimer-vacancies and two As dimers per unit cell (Chadi 1987; Farrell & Palmstrom 1990). The c(2 × 8) structure is simply a different arrangement of (2 × 4) unit cells on the surface. The GaAs(001)-(2 × 4) surface usually consists of a mixture of (2 × 4) and c(2 × 8) ordering (Pashley *et al.* 1988). Figure 1 shows an STM image of the GaAs(001)-(2 × 4)/c(2 × 8) surface with two dimer-vacancies per unit cell. The dark bands running from top left to bottom right are the dimer-vacancy rows.

The stability of the dimer-vacancy (2 × 4) structures can be understood in terms of electron counting (Pashley 1989), which requires that there are exactly the correct number of electrons in the surface layer fill all As dangling bonds and leave all Ga dangling bonds empty. If the As terminated surface had a complete layer of As dimers, there would be insufficient electrons available to fill all the As dangling bonds. It is only by introducing As dimer-vacancies (either one or two per unit cell) that this electron counting condition can be satisfied. One consequence of satisfying the electron condition is that there should be no states in the gap of the ideal

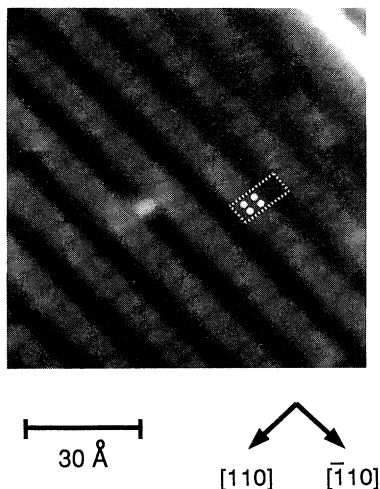


Figure 1. A filled state STM image of the $(2 \times 4)/c(2 \times 8)$ GaAs(001) surface reconstruction with two As dimers per unit cell. One unit cell ($8 \text{ \AA} \times 16 \text{ \AA}$) is marked on the image, together with the locations of the As atoms in the unit cell.

GaAs(2×4)/ $c(2 \times 8)$ surface, and hence no Fermi-level pinning. A full discussion of the structure of the GaAs(001)-(2×4)/ $c(2 \times 8)$ surface is given by Pashley & Haberern (1993).

3. Experimental

All samples discussed in this paper were grown by MBE under normal arsenic rich growth conditions at a temperature of approximately $580 \text{ }^\circ\text{C}$. N-type samples were grown in an *in situ* MBE chamber directly connected to the STM chamber. Epilayers were grown on GaAs(001) n^+ substrates, and doped with Si from a Si effusion cell. The growth was monitored by reflection high energy electron diffraction (RHEED) showing the surface to have a (2×4) reconstruction during growth. On completion of growth the samples were left to recover for two minutes in an As flux at the growth temperature. The samples were then rapidly removed from the growth chamber into the UHV preparation chamber and then transferred into the STM analytical chamber. The samples were under UHV conditions at all times. At room temperature, low energy electron diffraction (LEED) showed that the (2×4) surface reconstruction had been preserved. STM images were all taken at room temperature with a tunnelling current of 0.1 nA . The STM showed that this sample preparation technique (i.e. these growth conditions together with the rapid quenching to room temperature) produced a (2×4) surface with two As dimers and two dimer-vacancies per unit cell (Pashley & Haberern 1993).

P-type samples were grown in a separate MBE system under the same growth conditions as the n-type samples. They were grown on GaAs(001) p^+ substrates and doped with Be. On completion of growth the samples were cooled to room temperature in an As flux, producing a protective As capping layer on the surface. The samples were then transferred through air to the STM UHV system. The capping layer was removed by heating the samples up to the growth temperature in an As flux inside the *in situ* growth chamber. The decapping procedure was monitored by RHEED and found to produce a good (2×4) RHEED pattern. The p-type samples were then quenched to room temperature and transferred to the STM chamber in exactly

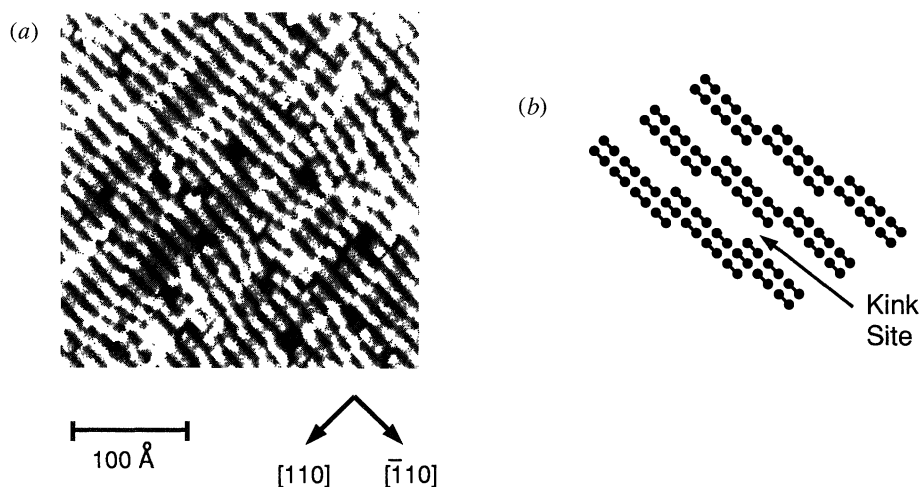


Figure 2. (a) A filled state STM image of the $(2 \times 4)/c(2 \times 8)$ GaAs(001) surface of a sample doped 10^{19} cm^{-3} with Si. The image was taken with -1.8 V on the sample. (b) Schematic of the kink structure with only the surface layer As atoms shown.

the same way as for the n-type samples. LEED showed that the (2×4) reconstruction was preserved and STM again showed that the (2×4) unit cell had two As dimers and two dimer-vacancies.

Scanning tunnelling spectroscopy (STS) was performed using the techniques developed by Feenstra & Stroscio (1987) and Mårtensson & Feenstra (1989). The major feature of the technique is that the tip is moved in towards the surface as the magnitude of the tunnelling voltage is decreased during acquisition of the $I-V$ curve. This provides improved dynamic range to the spectrum, enhancing information close to the band gap. A lockin amplifier is used to simultaneously record the differential conductivity (dI/dV) as a function of the applied voltage. The data are normalized by computing $(dI/dV)/(\bar{I}/\bar{V})$. This quantity gives a measure of the state density that is approximately independent of the tip-sample separation, and emphasizes spectral features close to and within the band gap. For a more detailed discussion on the spectroscopy technique as applied to these samples see Pashley *et al.* (1992).

4. Formation of surface acceptors on n-type GaAs(001)

It has been found that the GaAs(001)- $(2 \times 4)/c(2 \times 8)$ surface is strongly influenced by high levels of Si doping. The STM image of figure 1a shows the surface of lightly n-doped (approximately $3 \times 10^{17} \text{ cm}^{-3}$ Si) GaAs. The surface is well ordered with the dimer-vacancy rows running straight, over the entire image. This is in contrast to the surface of highly n-doped GaAs as shown in figure 2a where the doping level is approximately 10^{19} cm^{-3} Si. In this case, the surface is not nearly so well ordered, with the dimer-vacancy rows only being straight for a few unit cells. They regularly shift over by one atomic spacing (4 \AA), forming kinks in the dimer-vacancy rows. At this doping level the density of kinks is high, in excess of 10^{13} cm^{-2} . A schematic of the kink structure can be seen in figure 2b. The kinks are associated with the surface reconstruction, so exist only on the surface, and do not alter the bulk structure. The origin of these kinks turns out to be the key to understanding Fermi-level pinning on the clean GaAs(001) surface.

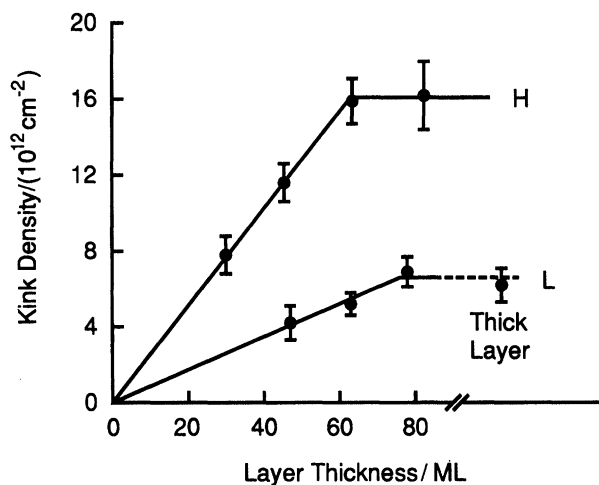


Figure 3. The density of kinks in the dimer vacancy rows, as determined from STM images, as a function of the thickness (in monolayers) of a Si doped GaAs(001) layer grown on top of an undoped buffer layer. Results are plotted for two Si concentrations, $3.4 \times 10^{18} \text{ cm}^{-3}$ and 10^{19} cm^{-3} (L and H respectively). The thickest layer for the L doping level is a few depletion widths thick. (After Pashley & Haberern 1991.)

The formation of these kinks as a function of the sample doping is illustrated in figure 3. In experiments by Pashley & Haberern (1991), samples were grown with an initial undoped buffer layer. No kinks in the dimer-vacancy rows were observed on these samples. On top of this buffer layer, a thin doped layer was grown. The kink density on the surface of the doped layer was determined from STM images as a function of the layer thickness. It was found that the kink density initially rises linearly with layer thickness for a given doping level (see figure 3). At a thickness of a few tens of monolayers ($1 \text{ ML} = 2.8 \text{ \AA}$) the kink density saturates and then remains constant for further increase in layer thickness. As the doping level is reduced, the saturation kink density reduces, and the critical thickness at which the saturation density is reached increases.

We can explain these results by associating the kinks with surface acceptor states which form so as to minimize the electronic energy of the surface region. This is most easily understood by considering the following 'thought experiment'. We start with perfectly flat band conditions right up to the surface in our doped layer. The Fermi-level will lie close to E_c , and electrons from the Si donor atoms will be in the conduction band. If we now create one acceptor state (a kink) at the surface with its energy level somewhere in the band gap, an electron can drop from the conduction band into this new state (figure 4*a*). This lowers the total energy of the system by the difference in energy between the Fermi-level (approximately E_c) and the acceptor state energy. This process can be continued by creating more acceptor states. The energy cost of this process comes from the surface charge accumulation that occurs as electrons have to come from further below the surface. This has the effect of bending the bands up at the surface, with the result that at the surface, the Fermi-level starts to move down in the band gap (figure 4*b*). This process can continue until the surface Fermi-level reaches the acceptor state (figure 4*c*). At this point, the energy gained by an electron dropping into the acceptor state is equal to the energy required to bring the electron up to the surface against the surface dipole that has

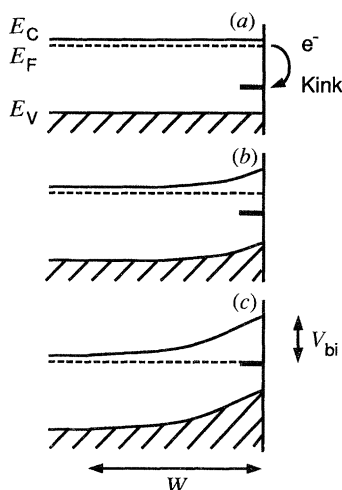


Figure 4. The mechanism of kink formation, which pins the Fermi-level close to mid gap. E_C , E_F , E_V are the conduction band minimum, Fermi-level, and valence band maximum respectively, W is the depletion width, and V_{bi} is the surface band bending.

been created. All the free electrons coming from the Si donor atoms within a depletion width of the surface are now in acceptor states at the surface. In this model, for a thick film, exactly the required number of surface acceptor states (kinks) are formed to bring the Fermi-level down to the acceptor level. This type of self-compensation mechanism therefore requires that the surface state density must equal the number of donors per unit area within the depletion width.

We can now consider the results of figure 3 in terms of this model of surface acceptor state formation. We begin by assuming that the mechanism occurs for all n-doping levels, so that the surface Fermi-level is always pinned to the acceptor state. At very low doping levels the Fermi-level approaches mid-gap in the bulk. For doping levels of 10^{17} cm^{-3} and above, the bulk Fermi-level is close to E_C and so the band bending is approximately constant. On nominally undoped material (in reality very low doped n-type material), the required kink density to bring the Fermi-level to mid gap is sufficiently low, that there are no kinks visible in a single STM image (figure 1a). As a doped layer is grown on top, more surface acceptor states, and hence kinks, are required to keep the Fermi-level pinned to the acceptor state. While the doped layer thickness is less than the depletion width for the doped layer, the entire layer is depleted. Part of the buffer layer is also depleted, but since its doping level is so low, it has a negligible effect on the surface kink density. As the layer thickness increases, the kink density rises proportionally. When the doped layer thickness exceeds W , the kink density remains constant for further increase in film thickness. Therefore, the layer thickness at which the saturation kink density occurs (figure 3) corresponds to the depletion width of the doped layer.

So far we have ignored one important energy term – the formation energy of the kink. Although the detailed atomic structure of the dimer-vacancy row at the kink site is not known, it is found that possible kink site structures do not satisfy the electron counting condition (see Pashley & Haberern (1993) for a more detailed discussion). The uncharged kink will be high in energy and so unstable. It is only by introducing additional charge at the kink site that the electron counting condition can be satisfied. Structural considerations suggest that the formation energy of a

charged kink site should be low. The fact that these kinks form in large numbers indicates that this is indeed correct. Hence from electron counting we can understand, in simple terms, why such a kink structure should be an acceptor.

Having related the electronic properties of the surface to particular structural features, it still remains to verify some of the assumptions that have been made. The first of these is to verify that charge is localized at the kink sites, and second that the surface Fermi-level lies somewhere in the band gap. STM together with tunnelling spectroscopy has been able to verify both of these issues.

The STM image is made up from both topographic and electronic components since it provides a spatial image of the local density of states. Closer examination of the STM image of the kinks on the surface of highly doped GaAs (figure 2*a*) reveals that the (2×4) unit cells adjacent to the kinks appear a little brighter (i.e. higher) than the unit cells away from the kinks. By imaging kinks at both positive and negative polarities (i.e. imaging empty and filled states), it is apparent that this is an electronic effect. If the effect was topographic, the apparent height change would be the same in both polarities. It is found that unit cells adjacent to kink sites appear brighter in filled state images and darker in empty state images (Pashley *et al.* 1992). This is a clear indication of the localization of negative charge at the kink sites (Stroscio & Feenstra 1988; Pashley *et al.* 1992). It is possible to quantify the amount of localized charge at each kink site by measuring the apparent height change adjacent to the kink. Following the technique developed by Stroscio & Feenstra (1988), this was calculated by Pashley *et al.* (1992) and found to be 1.2 ± 0.4 electrons. It is important to emphasize that this charge determination relies only on the local STM observation of the kink, and not on the measurement of kink density or doping level. The charge per kink at the surface can also be determined from the data of figure 3, where the doping level, depletion width and kink density are known. This gives a charge per kink site of 1.1 ± 0.2 electrons. These two independent charge determinations are in very good agreement and are consistent with each kink site being a single acceptor.

The position of the surface Fermi-level is directly determined from tunnelling spectroscopy. When zero volts are applied between the tip and the surface, the metal and semiconductor Fermi-levels line up. The spectrum shown in figure 5*a* is the average of several spectra taken from on top of the As dimers on the surface of a sample doped n-type with 10^{19} cm^{-3} Si. The valence and conduction bands are clearly seen with a well-defined band gap between them. The band gap measured approximately 1.4 eV in agreement with the expected bulk band gap. The Fermi-level (i.e. 0V) lies very close to mid gap. Averaging over many data-sets, the position of the Fermi-level is found to be $E_v + (0.7 \pm 0.1)$ eV. The Fermi-level is independent of position on the surface within the accuracy of the measurement. Tunnelling spectroscopy therefore confirms that the Fermi-level is in the middle of the band gap, consistent with the model for the pinning mechanism, and consistent with the Fermi-level position determined for n-type GaAs(001) by other techniques (Mao *et al.* 1992). The only band gap states that have been observed by STS at kink sites, are tails coming in from the band edges. Whether these tails of states are responsible for the pinning, or whether there are mid gap states that STS does not see, remains an open question (see Pashley *et al.* 1992).

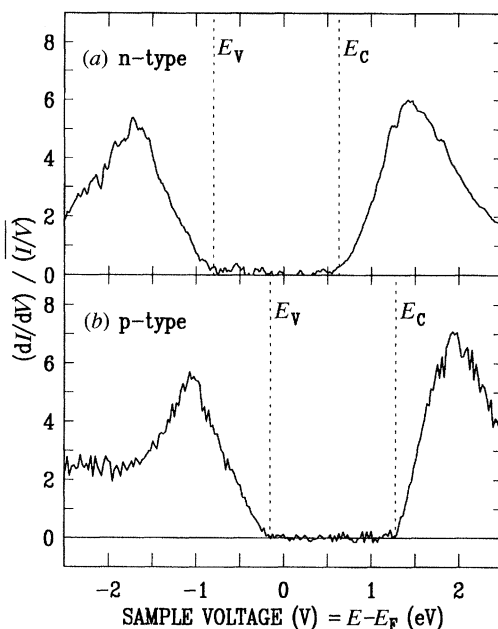


Figure 5. Tunnelling spectrum taken from on top of the As dimers on (a) an n-type GaAs(001)-(2 × 4)/c(2 × 8) surface with the sample doped with 10^{19} cm^{-3} Si (from Pashley *et al.* 1992) and (b) a p-type GaAs(001)-(2 × 4)/c(2 × 8) surface with the sample doped with 10^{19} cm^{-3} Be (from Pashley *et al.* 1993).

5. p-type GaAs(001)

The electronic properties of the p-type GaAs(001) surface is significantly different from the n-type surface. The STM shows that at a p-doping level of 10^{19} cm^{-3} Be, there is no significant number of kinks in the dimer-vacancy rows of the (2 × 4) reconstruction, and the surface is generally quite well ordered (see Pashley *et al.* 1993). There is no obvious surface defect or rearrangement that might be a surface donor and be responsible for pinning the Fermi-level close to mid gap. Tunnelling spectroscopy shows that at this high doping level, the Fermi-level is not close to mid gap. The spectrum shown in figure 5b, taken from an average of spectra on top of the As dimers, shows the Fermi-level to be within 150 meV of the valence band edge. The band gap is again close to the bulk band gap, as seen on n-type surfaces.

It is clear that the Fermi-level on these p-type samples is not pinned at mid gap as in the case of the n-type samples. However, the spectrum does indicate some band bending at the surface: the Fermi-level remains 150 meV above E_v and the spectra show no indication of a dopant induced current in the band gap as is seen on the flat-band GaAs(110) surface (Feenstra & Stroscio 1987). The likely origin of this band bending will be discussed below. Due to the high doping level and the observation of the bulk band gap in the spectra, it is not a tip induced effect.

6. Discussion

The STM results described above have shown that on n-type GaAs(001) surface acceptor states (kinks in the dimer-vacancy rows) form in exactly the required numbers to keep the Fermi-level pinned at mid gap irrespective of the doping level.

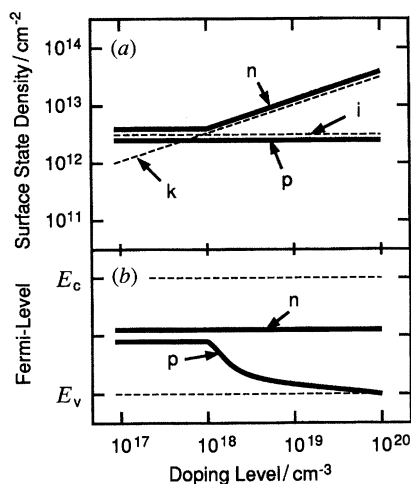


Figure 6. The Fermi-level pinning behaviour of n- and p-type GaAs(001) showing (a) surface state density and (b) Fermi-level as a function of doping level. Also plotted are the intrinsic defect state density (i) and the surface state density required to keep the Fermi-level at mid gap (k).

In contrast, there is no evidence for the formation of surface donors on p-type GaAs(001), and at high doping levels the Fermi-level is found to be close to the valence band.

The STM images of both these surfaces show there to be a considerable number of defects of various types on the surface, including 'missing' unit cells and step edges. No detailed studies have been made of the electronic properties of these defects, but it is likely that these will introduce some states within the band gap. The density of these states is hard to quantify without a more detailed knowledge of their structure, but it could be at least 10^{12} cm^{-2} on many of the samples imaged by STM, and will be dependent on growth conditions and sample preparation technique.

We now consider the role that these intrinsic defects play in Fermi-level pinning on n- and p-type material. The surface state density that is required to bring the Fermi-level to mid gap for both n- and p-type material is given by the depletion approximation (see Sze 1981), and is plotted as a function of doping level in figure 6a. Also plotted in figure 6a is the density of intrinsic surface states, which is assumed to be constant at all doping levels, and in this case assumed to be $3 \times 10^{12} \text{ cm}^{-2}$. On n-type material we have seen that kinks form so as to maintain enough surface states to keep the Fermi-level at mid gap. So for high doping levels where the kink density is higher than the intrinsic surface state density, the intrinsic defects play no role. At lower doping levels the intrinsic defects provide enough surface states to pin the Fermi-level. It is assumed that under these conditions there should be no energetic reason for kink formation. The surface state density and the Fermi-level position as a function of doping level for n-type material are shown in figure 6. The Fermi-level is pinned at mid gap for all doping levels.

In the case of p-type material, it is only the intrinsic defects that provide surface states to pin the Fermi-level. At low doping, the surface state density is sufficient to pin the Fermi-level close to mid gap (figure 6a). However, at higher doping levels the density is insufficient to bring the Fermi-level up to mid gap. The Fermi-level will therefore 'float' and be dependent upon the intrinsic defect density. As the doping level increases, the Fermi-level moves down towards E_v . In the p-type samples

discussed above with 10^{19} cm^{-3} Be doping the Fermi-level was found to be close to the valence band, consistent with an intrinsic defect density of about $3 \times 10^{12} \text{ cm}^{-2}$. Recently published photoemission results by Mao *et al.* (1992) for GaAs(001) doped p-type with approximately 10^{18} cm^{-3} Be show the Fermi-level to vary between $E_v + 0.4 \text{ eV}$ and $E_v + 0.6 \text{ eV}$. This is again consistent with an intrinsic defect density in the low 10^{12} cm^{-2} range (figure 6*b*).

From a technological point of view, the conclusions are clear. The surface of n-type GaAs will always be pinned at mid gap irrespective of doping level. P-type material, on the other hand, provides the possibility of unpinning the surface Fermi-level by increasing the doping. What happens when another material is deposited on the GaAs(001) surface is another issue. In many cases this may introduce states within the band gap that dominate the pinning process. Recent photoreflectance measurements by Yin *et al.* (1992) show a difference in pinning behaviour between n- and p-type GaAs(001) surfaces that have been exposed to air. This may indicate that the influence of the clean surface is still important when adsorbed layers are present.

7. Summary

STM results have shown that Fermi-level pinning on the GaAs(001)-(2 × 4) surface of n-type material occurs due to the formation of kinks in the dimer-vacancy rows of the (2 × 4) reconstruction. It has been determined that these kinks are single acceptor states and form in exactly the correct number to keep the Fermi-level at mid gap irrespective of doping level. At low n-doping levels intrinsic defects such as step edges may pin the Fermi-level.

On p-type material it is only the intrinsic defects that are responsible for Fermi-level pinning. Since the intrinsic defect density will depend upon growth conditions, among other factors, the Fermi-level position will be sample dependent. At high doping levels the Fermi-level is found to be close to the valence band. At low doping levels the Fermi-level on p-type material will be pinned close to mid gap.

I acknowledge R. M. Feenstra, K. W. Haberern and P. D. Kirchner, who were directly involved with the work discussed in this review. I am also grateful to T. Marshall, C. Van de Walle and J. M. Woodall for many fruitful discussions.

References

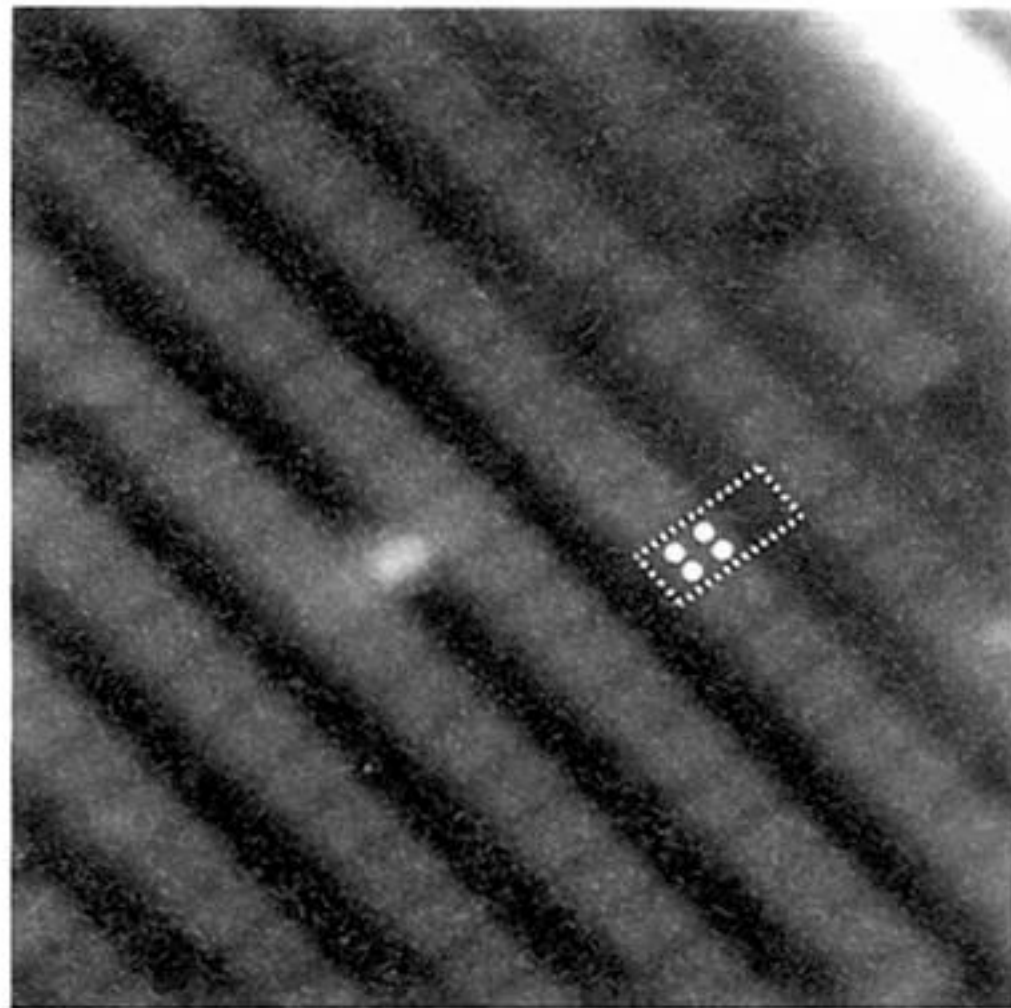
- Chadi, D. J. 1987 Atomic structure of GaAs(100)-(2 × 1) and (2 × 4) reconstructed surfaces. *J. Vac. Sci. Technol. A* **5**, 834–837.
- Drathen, P., Ranke, W. & Jacobi, K. 1978 Composition and structure of differently prepared GaAs(100) surfaces studied by LEED and AES. *Surf. Sci.* **77**, L162–L166.
- Farrell, H. H. & Palmstrom, C. J. 1990 Reflection high energy electron diffraction characteristic absences in GaAs(100) (2 × 4)-As: A tool for determining the surface stoichiometry. *J. Vac. Sci. Technol. B* **8**, 903–907.
- Feenstra, R. M. & Stroscio, J. A. 1987 Tunneling spectroscopy of the GaAs(110) surface. *J. Vac. Sci. Technol. B* **5**, 923–929.
- Hecht, M. H. 1990 Role of photocurrent in low-temperature photoemission studies of Schottky-barrier formation. *Phys. Rev. B* **41**, 7918–7921.
- Mao, D., Kahn, A., Le Lay, G., Marsi, M., Hwu, Y. & Margaritondo, G. 1992 Kelvin probe and synchrotron radiation study of surface photovoltage and band bending at metal/GaAs(100) interfaces. *Appl. Surf. Sci.* **56–58**, 142–150.
- Mårtensson, P. & Feenstra, R. M. 1989 Geometric and electronic structure of antimony on the GaAs(110) surface studied by scanning tunneling microscopy. *Phys. Rev. B* **39**, 7744–7753.

- Pashley, M. D. 1989 Electron counting model and its application to island structures on molecular-beam epitaxy grown GaAs(001) and ZnSe(001). *Phys. Rev. B* **40**, 10481–10487.
- Pashley, M. D. & Haberern, K. W. 1991 Compensating surface defects induced by Si doping of GaAs. *Phys. Rev. Lett.* **67**, 2697–2700.
- Pashley, M. D. & Haberern, K. W. 1993 The role of surface reconstructions in MBE growth of GaAs. In *Semiconductor Interfaces at Sub-nanometer Scale*, (ed. H. W. M. Salemink & M. D. Pashley), pp. 63–74. NATO ASI Series E no. 243. (Dordrecht: Kluwer.)
- Pashley, M. D., Haberern, K. W. & Feenstra, R. M. 1992 Tunneling spectroscopy on compensating surface defects induced by Si doping of molecular-beam epitaxially grown GaAs(001). *J. Vac. Sci. Technol. B* **10**, 1874–1880.
- Pashley, M. D., Haberern, K. W., Feenstra, R. M. & Kirchner, P. D. 1993 Different Fermi-level pinning behavior on n- and p-type GaAs(001). *Phys. Rev.* **B48**.
- Pashley, M. D., Haberern, K. W., Friday, W., Woodall, J. M. & Kirchner, P. D. 1988 Structure of GaAs(001) (2×4) – $c(2 \times 8)$ determined by scanning tunneling microscopy. *Phys. Rev. Lett.* **60**, 2176–2179.
- Rhoderick, E. H. & Williams, R. H. 1988 *Metal–semiconductor contacts*. (252 pages.) Oxford; Clarendon Press.
- Spicer, W. E., *et al.* 1988 The advanced unified defect model for Schottky barrier formation. *J. Vac. Sci. Technol. B* **6**, 1245–1251.
- Strosio, J. A. & Feenstra, R. M. 1988 Scanning tunneling spectroscopy of oxygen adsorbates on the GaAs(110) surface. *J. Vac. Sci. Technol. B* **6**, 1472–1478.
- Sze, S. M. 1981 *Physics of semiconductor devices*, pp. 74–84. New York: Wiley.
- Vituro, R. E., *et al.* 1989 Low-temperature formation of metal/molecular-beam epitaxy-GaAs(100) interfaces: approaching ideal chemical and electronic limits. *J. Vac. Sci. Technol. B* **7**, 1007–1012.
- Yin, X., *et al.* 1992 Photoreflectance study of the surface Fermi level at (001) n- and p-type GaAs surfaces. *J. Vac. Sci. Technol. A* **10**, 131–136.

Discussion

G. P. SRIVASTAVA (*University of Exeter, U.K.*). The STM images have clearly shown the (2×4) and $c(2 \times 8)$ reconstructions of the GaAs(001) surface. It has been claimed in the past by Feenstra and co-workers that voltage-dependent STM imaging can be used to deduce atomic positions inside the unit cell of the GaAs(110) surface when it is clean as well as when it is covered with an ordered monolayer deposition of Sb. Can the atomic positions in the unit cells for the above reconstructions of the GaAs(001) surface be deduced, and with what degree of accuracy?

M. D. PASHLEY. The STM does not directly image atomic positions. It images the local density of states as a function of position on the surface, with the energy of the states that contribute to the image being dependent on the voltage between the tip and the sample. The work of Feenstra and co-workers on GaAs(110) required theoretical calculations to compare with the STM images to derive information on the Ga–As surface buckling. In general, the STM will not give atomic positions to better than 1–2 Å. On the GaAs(001) surface, we can determine the atomic arrangement of As dimers in the unit cell, but cannot make any useful determination of the As–As dimer bond length.



30 Å

$[110]$ $[\bar{1}10]$

Figure 1. A filled state STM image of the $(2 \times 4)/c(2 \times 8)$ GaAs(001) surface reconstruction with two As dimers per unit cell. One unit cell ($8 \text{ \AA} \times 16 \text{ \AA}$) is marked on the image, together with the locations of the As atoms in the unit cell.

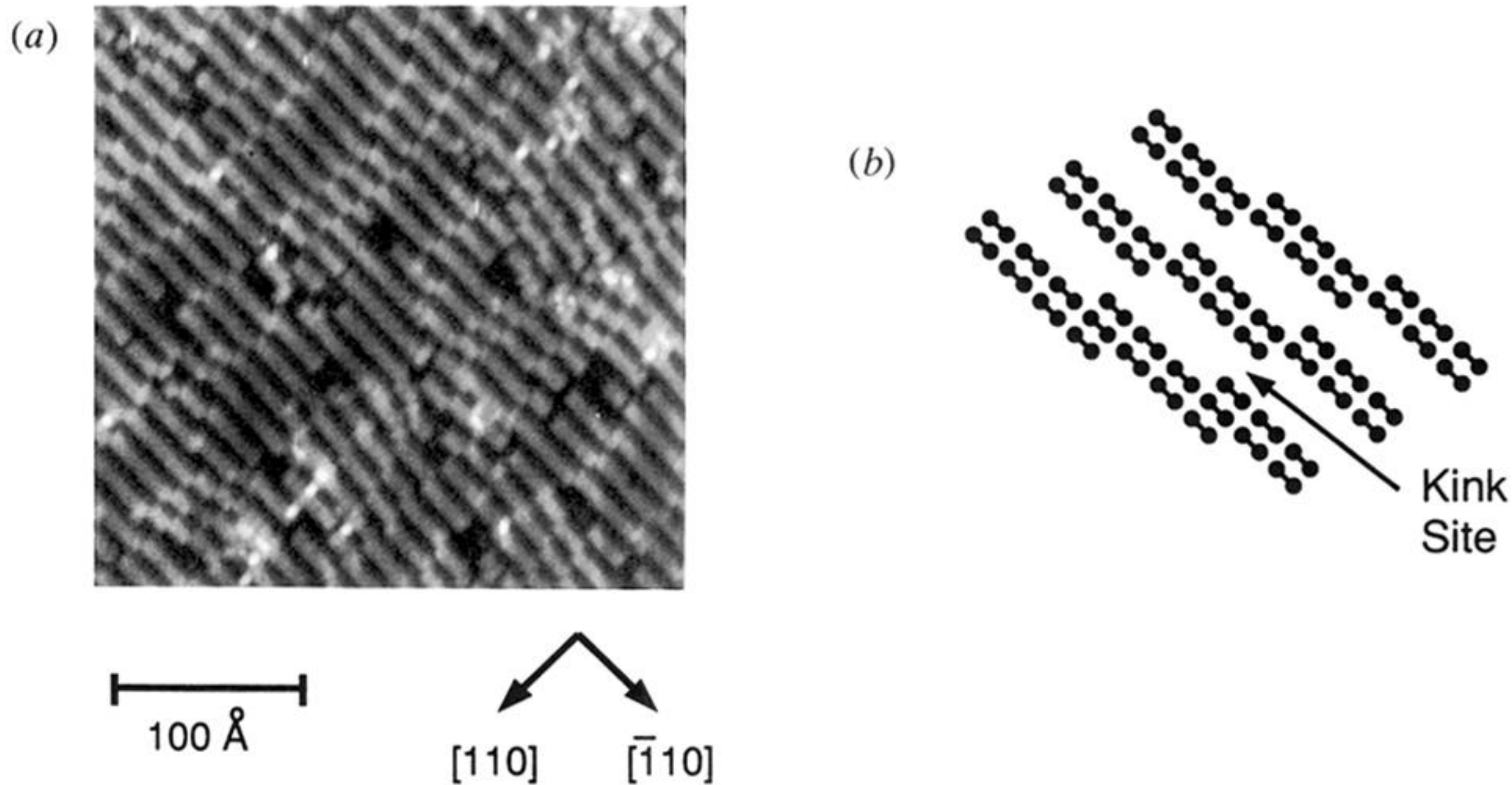


Figure 2. (a) A filled state STM image of the $(2 \times 4)/c(2 \times 8)$ GaAs(001) surface of a sample doped 0^{19} cm^{-3} with Si. The image was taken with -1.8 V on the sample. (b) Schematic of the kink structure with only the surface layer As atoms shown.